Eur. Phys. J. B **13**, 75–81 (2000)

THE EUROPEAN PHYSICAL JOURNAL B

EDP Sciences

Crystal-chemistry aspects and electric-field-gradient (EFG) dispersion in Ca-gallogermanate-type structures studied by Mössbauer spectroscopy

S. Constantinescu[a] and D. Tarina

National Institute for Materials Physics, P.O. Box Mg.-07, 76900 Bucharest, Romania

Received 3 February 1999

Abstract. The crystal field disorder in some trigonal germanates of the type $X_{3-y}Ln_yFe_{2+y}Ge_{4-y}O_{14}$ (X = Ba, Sr; Ln = La, Nd; y = 0, 1) is studied by ^{57}Fe Mössbauer effect. The dispersion of the electric field gradient (EFG) at the octahedral sites of these compounds is investigated. A correlation of the experimental and calculated EFG data with some crystal-chemistry aspects is presented.

PACS. 76.80.+y Mössbauer effect; other γ-ray spectroscopy

1 Introduction

Calcium gallium germanate, $Ca_3Ga_2Ge_4O_{14}$, characterized by the space group $P321$, is representative for a class of acentric crystals with structural static disorder of the crystal field [1]. The structure described in [2–4] consists of successive layers of $T1$ (position $3f$) and $T2$ (position $2d$) tetrahedra ($z/c \sim 0$), alternating along the c-axis with interlayers ($z/c \sim 0.5$) of large oxygen polyhedra, (octahedra Oh (position $1a$) and Thompson cubes (position $3e$) with the 8-coordinated cation site (A) occupied by Ca^{2+} ions (Fig. 1).

The interest for such structures derives from their lack of inversion centre combined with relatively large oxygen cages and crystal field disorder. Indeed, the large acentric oxygen polyhedra, which are suitable hosts for laser ions (*e.g.* Cr^{3+}, Nd^{3+}), show a crystal field dispersion owing to the random occupation of the neighboring $T1$ tetrahedral sites by the Ga^{3+} or Ge^{4+} ions. It was found [1] that systems having such activator centres occupying sites with slightly different crystal field (described by the "quasi-centre" concept) have specific spectroscopic and laser properties (*e.g.* the broad band tunable stimulated emission of Cr^{3+} ions in crystals with Ca-gallogermanate structure reported in [1]). The investigation of the crystal-field dispersion in these systems is therefore a subject of considerable interest.

In this paper a Mössbauer effect search for the electric field gradient (EFG) dispersion at the octahedral sites in some trigonal iron germanates is presented. The calculated and experimental EFG data are corralated with the crystal-chemistry aspects of the respective compounds.

[a] e-mail: sconst@alpha1.infim.ro or pcnet.pcnet.ro

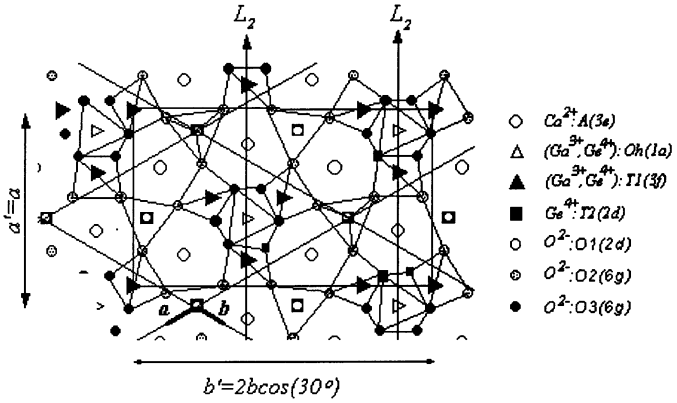

Fig. 1. Rectangular unit cell of the $Ca_3Ga_2Ge_4O_{14}$-type structure; projection on (001) plane [3].

2 Crystal-chemistry aspects of some Ca-gallogermanate type structures

The trigonal germanates of the type $X^{2+}_{3-y}Ln^{3+}_y$ $Y^{3+}_{2+y}Ge^{4+}_{4-y}O_{14}$ (X = Ba, Sr, Ca; Y = Fe, Ga; Ln = rare-earth; y = 0, 1), their synthesis and X-ray structural analysis are reported in [2–5]. In all the compounds the alkaline earth ($Ba^{2+}, Sr^{2+}, Ca^{2+}$) and rare earth ($Ln^{3+}$) ions enter the 8-coordinated sites of the Thompson cubes (A), while the other cations $Fe^{3+}(Ga^{3+})$ and Ge^{4+} are distributed over the octahedral or tetrahedral sites. As expected, the unit cell volume V depends on the weighted values $r^{\rm w}_8(A)$ of the radius of the 8-coordinated cation (A) (Tab. 1).

A linear decrease of V accompanied by a relative elongation of the unit cell along the c-axis as given by c/a

Table 1. The weighted values of radius $r_8^{\rm w}(A)$, of electronegativity $\chi^{\rm w}(A)$, and of the factor $F(A) = [\chi_{\rm P}(O) - \chi^{\rm w}(A)]^2$ for the 8-coordinated cation.

Compound	$r_8^{\rm w}(A)$[Å]	$\chi^{\rm w}(A)$	$F(A)$
$Ca_3Ga_2Ge_4O_{14}$	1.120	1.000	5.954
$Sr_2NdFe_3Ge_3O_{14}$	1.207	1.013	5.890
$Sr_2PrFe_3Ge_3O_{14}$	1.213	1.010	5.905
$Sr_2LaFe_3Ge_3O_{14}$	1.227	1.000	5.954
$Sr_3Ga_2Ge_4O_{14}$	1.250	0.950	6.200
$Ba_2LaFe_3Ge_3O_{14}$	1.340	0.960	6.150
$Ba_3Fe_2Ge_4O_{14}$	1.420	0.890	6.502

Here $r_8^{\rm w}(A) = \frac{1}{3}[r_8({\rm X})w({\rm X}) + r_8({\rm Ln})w({\rm Ln})]$, $\chi^{\rm w}(A) = \frac{1}{3}[\chi_{\rm P}({\rm X})w({\rm X}) + \chi_{\rm P}({\rm Ln})w({\rm Ln})]$ where r_8, $\chi_{\rm P}$ and w are the effective ionic radius [6], Pauling's electronegativity, and the weight of the 8-coordinated cation. $\chi_{\rm P}(O)$ is Pauling's electronegativity of oxygen ($\chi_{\rm P}(O) = 3.44$).

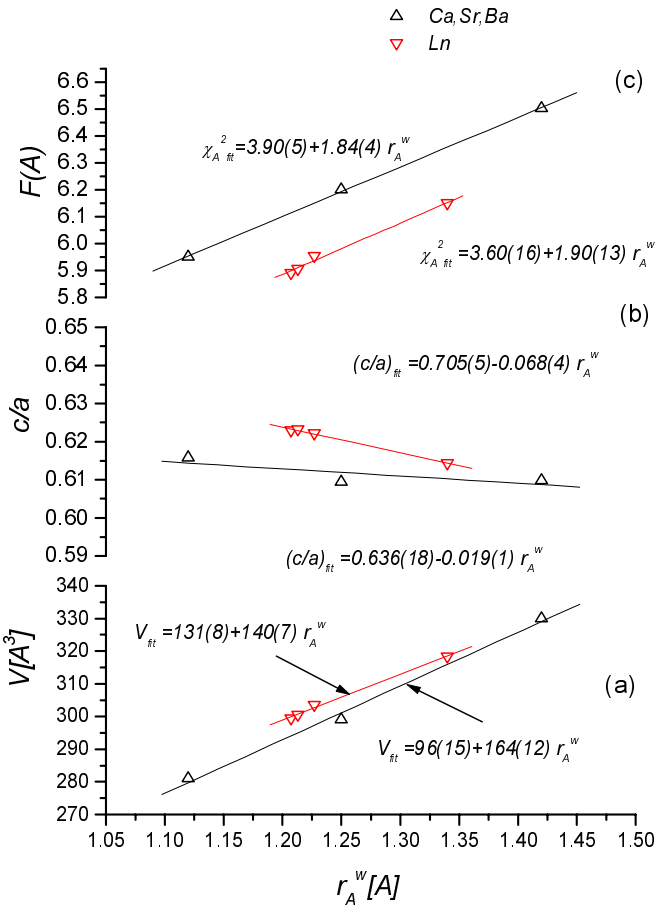

Fig. 2. Unit cell volume V (a), relative elongation c/a (b) and the factor $F(A)$ (c) for the compounds listed in Table 1. (The figures in parentheses give the standard deviations of the fitting coefficients.)

are observed when the Thompson cubes are occupied by cations of smaller size [2–5]. However, as one can be seen in Figures 2 and 2b, for the groups of compounds with or without rare earth ions, distinctly different V and c/a linear dependences are found, especially for the elongation c/a. This shows that beyond mere size effects, the type of ion plays also an important role in these systems. Considering the $\chi^{\rm w}(A)$ electronegativity values as an approximate measure of ionicity of the $A-O$ bonds [8], the expression $F(A)$ defined in Table 1 can be used to characterize the ionic character of the cation-oxygen bond energy in the Thompson cubes. A plot of the factor $F(A)$ *versus* $r_8^{\rm w}(A)$ (Fig. 2c) reveals the distinct difference between these compounds. For a given weighted radius value $r_8^{\rm w}(A)$, it seems that the respective $A-O$ bond energy in the Thompson cubes of (Ba, Sr, Ca) germanates is higher than that characterising the same polyhedra in the samples with the rare earth ions. This remark is in agreement with the results reported in [1] where a stronger octahedral crystal field was observed in the alkaline earth germanates at Cr^{3+} ions in comparison with the crystal field found for the same ions in the rare earth gallates.

Further information on crystal-chemistry aspects could be obtained owing to the presence of iron in the structure of some germanates. A previous Mössbauer spectroscopy study on the set of samples presented in Table 2 was performed by using ^{57}Fe isotope as spectroscopic probe [7]. A representative room temperature Mössbauer spectrum is given in Figure 3 for $Sr_2NdFe_3Ge_3O_{14}$ sample. In an initial stage, the spectra can be computer fitted and resolved into two quadrupole doublets of large Γ linewidths ($0.35 \div 0.5$ mm/s), typical for high spin Fe^{3+} ions in octahedral and respectively in tetrahedral environment. It was shown that Fe^{3+} ions are randomly distributed together with Ge^{4+} ions over the Oh octahedral and $T1$ tetrahedral sites, while the $T2$ tetrahedra remain occupied only by Ge^{4+} ions. In Table 2 are listed the computer fitted hyperfine parameters (isomer shift S, quadrupole splitting $\Delta^{\rm exp}$) characterizing the crystal chemistry and the symmetry of iron in the structure, as well as the iron occupancy x of the Oh and $T1$ sites, deduced from the corresponding spectral area ratios.

Analysing the data in Table 2 one sees that cation substitution in the Thompson cubes leads to changes in the crystal-chemistry features of the Oh and $T1$ sites and also in their cation occupancy. In Figure 4 the changes of $S(Oh)$ and $x(Oh)$ parameters are displayed in function of the factor $F(A)$. As the $F(A)$ value decreases (more electronegative cations A in Thompson cubes), a decrease of the isomer shift $S(Oh)$ is also observed (Fig. 4a), accompanied by an exponential increase of the iron occupancy $x(Oh)$ (Fig. 4b). It seems that a decrease of ionic bond energy in Thompson cubes should favour iron to enter the octahedral sites where the Fe-O bonds get a relatively less ionic character.

This finding is in agreement with the preference of Fe ions for sites with more covalent bonds, pointed out in a study on the olivine structure [8].

Table 2. Room temperature Mössbauer parameters and the corresponding chi- square values, $\chi^2_{\rm fit}$ of fitted spectra.

Sample	Notation	$\chi^2_{\rm fit}$	Site	[a] S[mm/s]	$\Delta^{\rm exp}$[mm/s]	$\Gamma^{\rm exp}$[mm/s]	[b] x
$Ba_3Fe_2Ge_4O_{14}$	Ba	2.75	*Oh*	0.390	0.96	0.37	0.72
			$T1$	0.265	1.85	0.57	1.28
$Sr_3Fe_2Ge_4O_{14}$	Sr	2.63	*Oh*	0.404	0.95	0.34	0.72
			$T1$	0.268	1.74	0.51	1.28
$Sr_2LaFe_3Ge_3O_{14}$	Sr(La)	2.12	*Oh*	0.361	0.91	0.40	0.84
			$T1$	0.288	1.81	0.60	2.16
$Sr_2NdFe_3Ge_3O_{14}$	Sr(Nd)	1.77	*Oh*	0.381	0.91	0.44	0.99
			$T1$	0.292	1.68	0.54	2.01
Errors				±0.005	±0.01	±0.02	±0.04

[a] Isomer shift S referred to metallic iron; [b] x values are calculated as in [7].

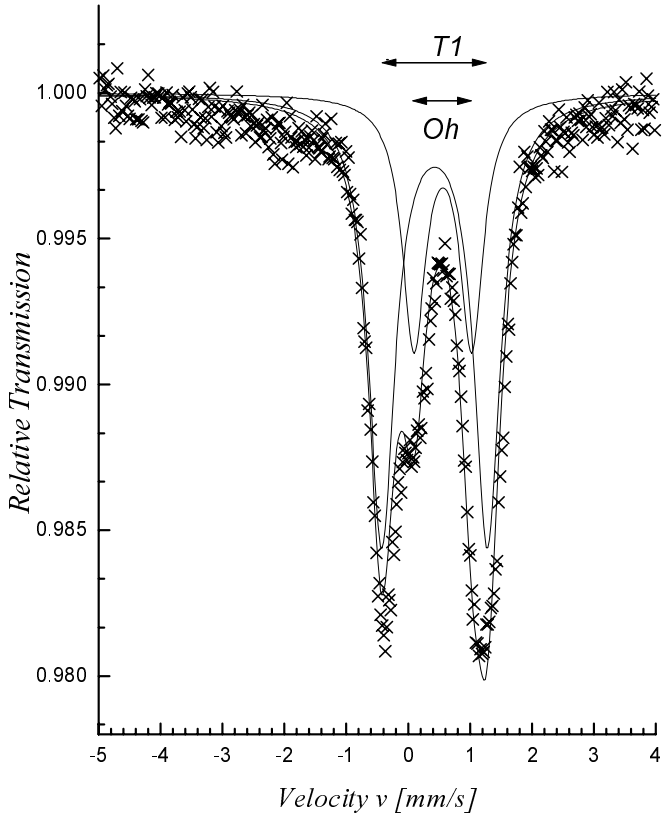

Fig. 3. Room temperature Mössbauer spectrum of $Sr_2NdFe_3Ge_3O_{14}$. Zero velocity is with respect to a ^{57}Co in chromium source.

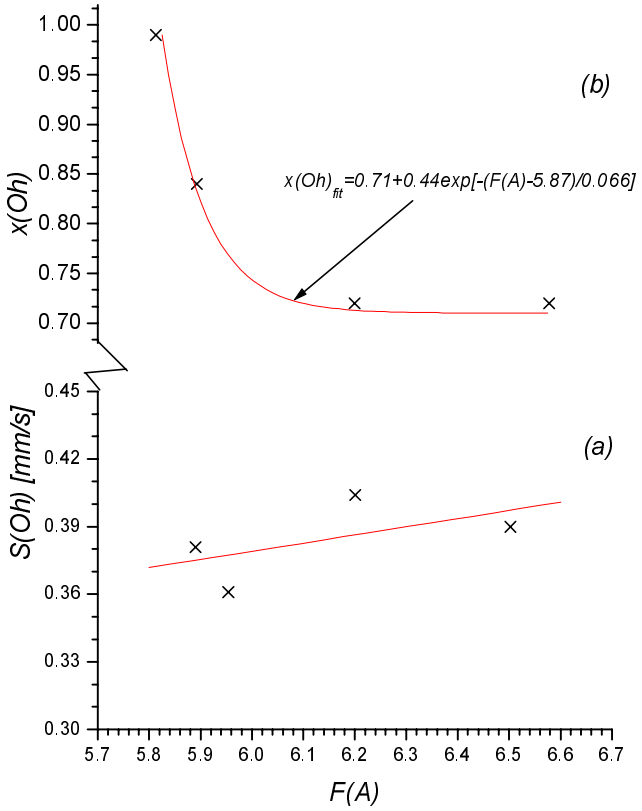

Fig. 4. Isomer shift $S(Oh)$ for octahedral Fe^{3+} ions and iron occupancy $x(Oh)$ *versus* the factor $F(A)$.

3 Electric-field-gradient (EFG) dispersion at the octahedral sites in Ba, Sr and Sr(Ln)-iron germanates

3.1 Experimental

According to the quadrupole splitting $\Delta^{\rm exp}$ and $S^{\rm exp}$ data in Table 2, both octahedra and tetrahedra are very distorted and occupied by HS ferric ions. Moreover, the very large Γ linewidths found for the spectral patterns show the presence of more crystallographically inequivalent *Oh* octahedral and $T1$ tetrahedral sites. Concerning the crystallographic inequivalence of the octahedra, this may be mainly due to the random occupation of their cation environment by more than one sort of ions, resulting in a dispersion of lattice electric field gradient at the *Oh* sites. To investigate this dispersion a deconvolution of the experimental spectra was attempted and the best fit (with $\chi'^2 \approx 0.75 \div 0.86\ \chi^2$) was obtained indeed, resolving

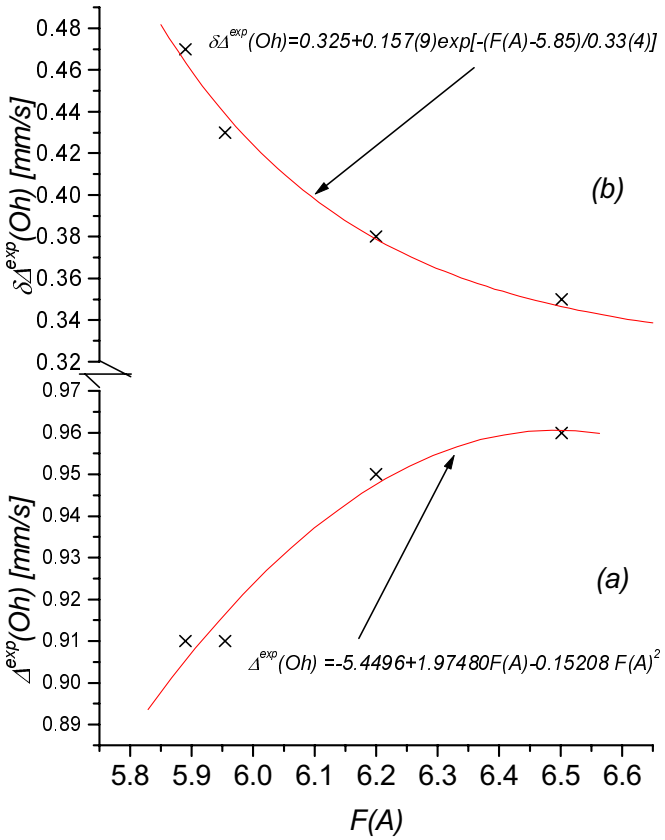

Fig. 5. Experimental quadrupole splitting $\Delta^{\exp}(Oh)$ (a) and its dispersion $\delta\Delta^{\exp}(Oh)$ (b) for octahedral iron species *vs.* the factor $F(A)$. (The figures in parentheses give the standard deviations of the fitting coefficients.)

the subspectrum for Fe in octahedra into three octahedral quadrupole doublets (Q_1, Q_2, Q_3) with the $\Delta^{\exp}(Q_i)$ parameters presented in Table 3.

The quantity $\delta\Delta^{\exp}(Oh) = [\Delta^{\exp}(Q_1) - \Delta^{\exp}(Q_3)]/2$ shows the width of the distribution of Oh species for a given sample and can be considered a measure of crystal field disorder over the respective sites. A plot of $\Delta^{\exp}(Oh)$ (Tab. 2) and of $\delta\Delta^{\exp}(Oh)$ (Tab. 3) *vs.* $F(A)$ is given in Figure 5.

Going from Ba to Sr(Nd) samples, the factor $F(A)$ decreases, and a decrease of the $\Delta^{\exp}(Oh)$ is also observed, that is the distortion of the respective octahedra decreases, while the corresponding EFG dispersion increases exponentially. For both $\Delta^{\exp}(Oh)$ and $\delta\Delta^{\exp}(Oh)$ parameters, stronger changes are observed when Ln^{3+} ion substitution takes place on the A site. This corroborates the above role of the type of substituting ion.

The effect of the A cations on the electric field gradient in octahedra may be due to their presence in the nearest cation environment of the Oh sites, as well as to the changes induced in the $T1$ cation occupancies of this environment, as one can see in Table 2. To support these experimental findings, a computation of the EFG tensor and of its dispersion over the Oh sites is performed and presented in the following two sections.

3.2 Lattice electric-field-gradient computation at the octahedral sites in Ba, Sr and Sr(Ln)-iron germanates

A computation of the lattice EFG tensor at the Oh sites in the Ba, Sr and Sr(Ln) iron germanates has been performed using the computer program QSCOMP [9], according to the procedure described in [10]. Supposing that the lattice is a distribution of N point ionic charges q_i with position vectors $\mathbf{r}_i(x_i, y_i, z_i)$, the components $V_{\alpha\beta}$ of the EFG tensor at $\mathbf{r}_o(x_o, y_o, z_o)$ are given by the well-known expressions:

$$V_{\alpha\beta} = (1 - \gamma_\infty) V_{\alpha\beta}^{\text{latt}} \tag{1}$$

$$V_{\alpha\beta}^{\text{latt}} = \frac{1}{4\pi\varepsilon_0} \sum_{i=1}^{N} \frac{q_i}{|\mathbf{r}_i - \mathbf{r}_o|^5} \times \begin{cases} [3(x_{\alpha i} - x_{\alpha o})^2 - |\mathbf{r}_i - \mathbf{r}_o|^2] \leftarrow \alpha = \beta \\ (x_{\alpha i} - x_{\alpha o})(x_{\beta i} - x_{\beta o}) \leftarrow \alpha \neq \beta \end{cases} \tag{2}$$

with

$$\mathbf{r}_i = (x_i^0 + la)\mathbf{i} + (y_i^0 + mb)\mathbf{j} + (z_i^0 + nc)\mathbf{k}, \quad (l, m, n = 0, \pm 1, \pm 2, \dots) \tag{3}$$

where γ_∞ is Sterheimer's antishielding factor [11], ε_o the vacuum electric permitivity, x_α and x_β are rectangular coordinates (x, y, z), $\mathbf{r}_i(x_i^o, y_i^o, z_i^o)$ designating the positions of the N_i^o charges q_i in the rectangular unit cell with lattice constants $a, b, c, (i = 1, 2, \dots N$ and $N = (2|l|+1)(2|m|+1)(2|n|+1)N_i^o)$. The coordinates x_i^o, y_i^o, z_i^o and the lattice constants a, b, c are taken from X-ray diffraction data [5]. The actual values for the charges q_i have been obtained by the valence summation procedure [12] described in [10]. The q_i data and the respective ion positions are listed in Table 4 for the first 20 neighbours of the Oh site. The matrix of the EFG tensor is provided by the subroutine GRADIENT and the principal components V_{xx}, V_{yy}, V_{zz} and the corresponding eigenvectors are obtained by the diagonalisation subroutine EIGEN. The program gives also the Euler's angle (φ, θ, ψ) between the principal axes of EFG tensor and the crystallographic axes. In the Table 5 the main component V_{zz}, the asymmetry parameter η and the corresponding $\Delta^{\text{calc}}(Oh)$ quadrupole splittings for the coordination spheres of radius $R = 3.9$ Å and $R = 3.75$ Å for Ba and respectively Sr germanates are presented. The satisfactory correspondence between the calculated $\Delta^{\text{calc}}(Oh)$ and the experimental $\Delta^{\exp}(Oh)$ (Tab. 2) values for all studied compounds shows the essential role of the local environment on the behaviour of the Mössbauer probe located on the octahedral sites.

3.3 Computation of the lattice EFG dispersion at the octahedral site in Ba, Sr and Sr(Ln)-iron germanates

As it was explained above, the crystallographic inequivalence of the octahedral sites in these structures studied is

Table 3. Hyperfine parameters of the distribution of Oh species. (The standard deviation for $\Delta^{\exp}(Q_i)$ is about 0.03 mm/s).

Sample	Oh	$\Delta^{\exp}(Q_i)$ [mm/s]	$\Gamma^{\exp}(Q_i)$ [mm/s]	$\delta\Delta^{\exp}(Oh)$ [mm/s]
Ba	Q_1	1.31		0.33
	Q_2	0.97	0.27	
	Q_3	0.65		
Sr	Q_1	1.40		0.38
	Q_2	0.98	0.29	
	Q_3	0.64		
Sr(La)	Q_1	1.46		0.43
	Q_2	0.93	0.31	
	Q_3	0.60		
Sr(Nd)	Q_1	1.48		0.47
	Q_2	0.92	0.32	
	Q_3	0.54		

Table 4. The fractional ionic charge values q_i, obtained by valence summation procedure, in the lattice of Ba and of Sr iron germanates.

	Ba ($P3$ symmetry)			Sr ($P321$ symmetry)			Sr(La)	Sr(Nd)
N	R[Å]	Ions	q_i[v.u.]	R[Å]	Ions	q_i[v.u.]	q_i[v.u.]	q_i[v.u.]
	0.00	$(Fe_xGe_{1-x}) : 1b$	3.321	0.00	$(Fe_xGe_{1-x}) : 1a$	3.280	3.269	3.111
I	2.00(2)	$3O_4$: $3d$	-1.830	1.920(5)	$6O_3$: $6g$	-1.836	-1.780	-1.778
	2.01(2)	$3O_5$: $3d$	-1.901					
II	3.32(1)	$6(Fe_{2-x}Ge_{1+x}) : 3d$	3.620	3.190(5)	$6(Fe_{2+y-x}Ge_{1-y+x}) : 3f$	3.579	3.284	3.313
III	3.61(1)	3Ba: $3d$	2.035	3.50(1)	$3(Sr_{3-y}Ln_y) : 3e$	2.020	2.355	2.358
IV	3.88(1)	$3O_3$: $3d$	-2.177	3.74(1)	$6O_2$: $6g$	-2.232	-2.265	-2.256
	3.900(5)	$3O_2$: $3d$	-2.222					

Table 5. The calculated EFG data, the quadrupole splitting $\Delta^{\text{calc}}(Oh)$ and its dispersion $\delta\Delta^{\text{calc}}(Oh)$.(The standard deviations for $\Delta^{\text{calc}}(Oh)$ and $\delta\Delta^{\text{calc}}(Oh)$ are about 0.05 and respectively 0.03 mm/s.)

Sample	$V_{zz}[10^{20}V/m^2]$	η	$\Delta^{\text{calc}}(Oh)$ [mm/s]	$\delta\Delta^{\text{calc}}(Oh)$ [mm/s]
Ba	4.1799	0.09	0.94	0.28
Sr	4.8076	0.02	1.08	0.37
Sr(La)	3.8998	0.03	0.87	0.44
Sr(Nd)	3.9616	0.03	0.89	0.45

mainly due to a random occupation of the local environment with heterovalent cations. The resulting crystal-field disorder at these sites can be accounted for using a combinatorial occupation model applied to the three groups of cation sites in the first coordination sphere of Oh sites (see Tab. 4): three tetrahedral sites of $T1$ type located in the plane $z/c \sim 0$, the other three $T1$ sites located at $z/c \sim 1$ belonging to the upper cell and three Thompson cubes sites A at $z/c \sim 0.5$. Each group of sites is supposed to have independent random occupation of the type (Fe_xGe_{3-x}) and (Ln_yX_{3-y}) for $T1$ and A sites, respectively. The simultaneous random occupation probability of the three groups of sites is given by the relation

$$p(n,s) = \prod_{i=1}^{3} p_{N_i}^{n_i}(c_i) \tag{4}$$

where

$$p_{N_i}^{n_i}(c_i) = \frac{N_i!}{n_i!(N_i-n_i)!}\left(\frac{c_i}{3}\right)^{n_i}\left(1-\frac{c_i}{3}\right)^{N_i-n_i} \tag{5}$$

is the probability that in the cation neighbourhood (i) of the octahedral Fe^{3+} ion, the substituting element (Fe/Ln)

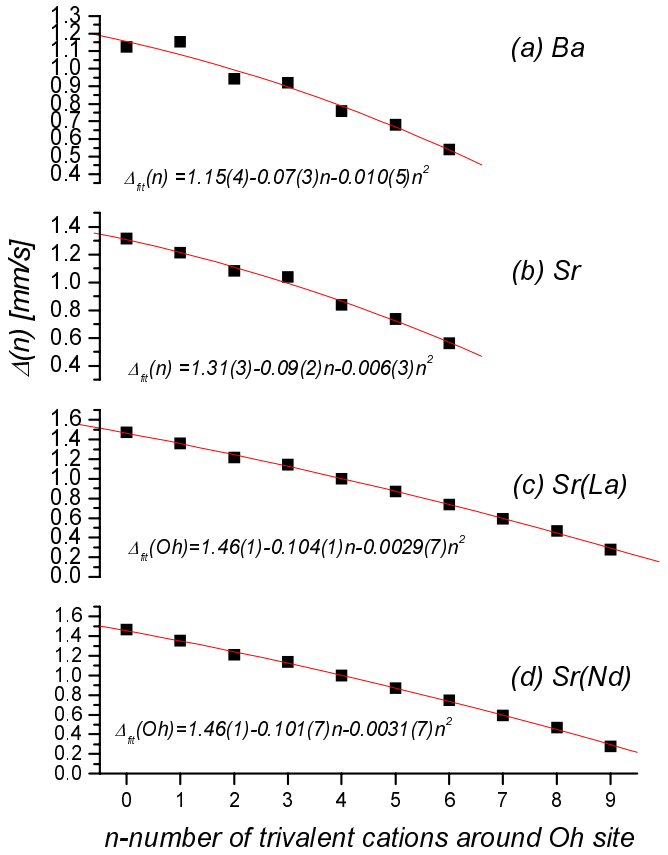

Fig. 6. The weighted mean values $\bar{\Delta}(n)$ of the quadrupole splitting as a function of the number n in Ba, Sr, Sr(La) and Sr(Nd) compounds. (Solid lines are fitted curves.)

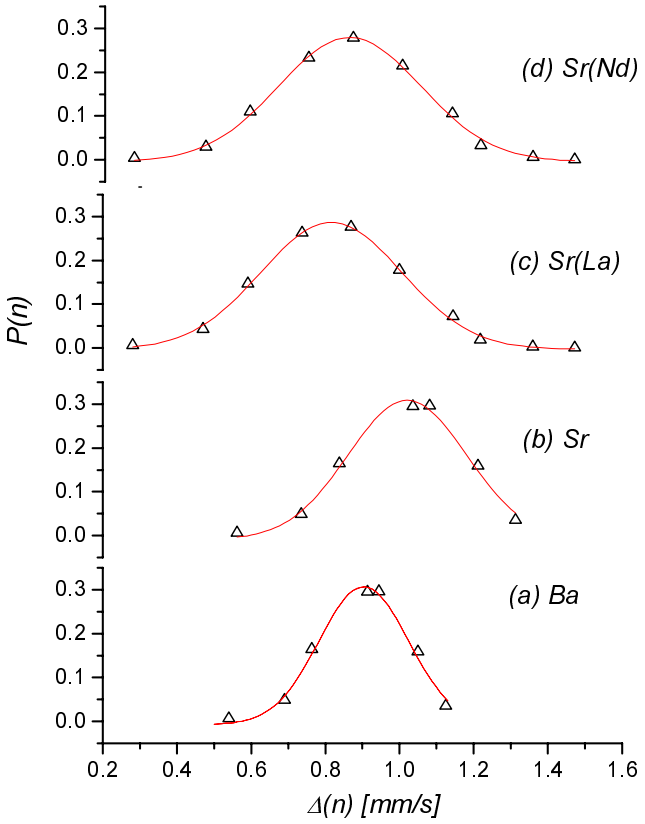

Fig. 7. The probabilities $P(n)$ of the quadrupole splitting $\bar{\Delta}(n)$ for Ba, Sr, Sr(La) and Sr(Nd) compounds. (Solid lines are fitted Gaussian curves.)

having the occupancy c_i (*i.e.* $x(T1)$ or $y(A)$ respectively) substitutes n_i sites from N_i possible ones (for all three groups (i) $N_i = 3$), n is given by the relation

$$n = \sum_{i=1}^{3} n_i \tag{6}$$

running from 0 to $n_{\max}$ and $s = 1, 2, \ldots k$, is a way of occupation from the k possible ones for a given n. Using the relations (4 – 6), the total random occupation probability $P(n)$ can be calculated as depending on the total number n of substituting trivalent cations in the first coordination sphere:

$$P(n) = \sum_{s=1}^{k} p(n, s). \tag{7}$$

Each way of occupation of the nearest cation environment (s) for a given n determines a certain lattice electric field gradient at the Oh site and consequently a certain value Δ_s of the Mössbauer quadrupole splitting with probability $p(n, s)$, [7,13]. For a given n, with k occupation ways, the quadrupole splitting has the weighted mean value

$$\bar{\Delta}(n) = \frac{\sum_{s=1}^{k} \Delta_s p(n, s)}{\sum_{s=1}^{k} p(n, s)} \tag{8}$$

with probability $P(n)$ as mentioned above. Thus the random occupation provides a dispersion of quadrupole splitting values. This dispersion is illustrated in Figure 6 for the Ba, Sr and Sr(Ln) compounds by plotting the calculated $\bar{\Delta}(n)$ values *vs.* the total number n of substituting trivalent cations in the first coordination sphere. A substantial change of the $\bar{\Delta}(n)$ value over the range of n is found in all cases. The difference $|\bar{\Delta}(0) - \bar{\Delta}(n_{\max})|$ is clearly larger when the A sites are also randomly occupied by heterovalent ions, like in Sr(Ln) compounds.

In Figure 7, the probabilities $P(n)$ of these quadrupole splittings $\bar{\Delta}(n)$ are plotted and fitted by Gaussian curves in order to obtain the $\delta\Delta^{\text{calc}}(Oh)$ dispersion data, as half linewidths, the $\bar{\Delta}(n)$ and the number of cations n corresponding to the highest $P(n)$ values.

The obtained $\delta\Delta^{\text{calc}}(Oh)$ data are listed in Table 5. Comparing the $\delta\Delta^{\text{calc}}(Oh)$ data with the spectral $\delta\Delta^{\text{exp}}(Oh)$ ones (Tab. 3), a satisfactory correspondence is remarked, which confirms the statistical model proposed for the crystal field disorder in these studied compounds.

As one can see from Figure 7 the Gaussian curves are shifted to smaller values of $\bar{\Delta}(n)$ in the presence of rare-earth cations on A sites. That corresponds to an increase of n.

4 Conclusions

In the trigonal germanates presented above, the crystal field disorder over the octahedral Oh sites is studied by a Mössbauer effect search for electric-field-gradient (EFG) dispersion at octahedral Fe^{3+} species. A computation of the EFG tensor and of its dispersion over the Oh sites is performed using the valence summation procedure and taking into account a combinatorial occupation model of the nearest cation environment of the octahedral iron. A satisfactory correspondence is found for all samples between the calculated EFG data and the experimental quadrupole splitting, $\Delta^{\exp}(Oh)$ as well as their dispersion $\delta\Delta^{\exp}(Oh)$, which proves the essential role of the local environment on the behaviour of the octahedral iron and the validity of the statistical model proposed. It was shown that both distortion, crystal chemical features, and cation occupancy of the local environment are substantially changed by the cation substitution in the 8-coordinated sites (Thompson cubes). Generally the presence of rare-earth cations in Thompson cubes suggests an incresing of $T1$-occupancy by trivalent ions and of the dispersion $\delta\Delta^{\exp}$ around Oh sites. Moreover, beyond size effect, the type of the substituting cation, its valence and electronegativity seem to be important. The changes in the octahedral iron occupancy $x(Oh)$, isomer shift $S(Oh)$, quadrupole splitting $\Delta(Oh)$ and dispersion $\delta\Delta(Oh)$ for the octahedral iron Fe^{3+} species are analysed as depending on the ionicity of the cation-oxygen bonds in Thompson cubes. It is found that as the weighted electronegativity of the 8-coordinated sites becomes higher, the octahedral Fe-O bonds become relatively less ionic in character and an exponential increase of the octahedral occupancy takes place. These changes are also accompanied by a decrease of the octahedral quadrupole splittings, *i.e.* of the distortion of the octahedra, while the corresponding $\delta\Delta(Oh)$ dispersion, *i.e.* the crystal-field disorder over the octahedral sites, increases exponentially. The last effect is much enhanced by the substitution of trivalent cations in the Thompson cubes.

References

1. A.A. Kaminskii, *Proc. 1st Int. School on Excited States of Transition Elements, Ksiaz Castle, 1988*, edited by B. Jezowska-Trzebiantowska, J. Legendziewicz, W. Strek (World Scientific Singapore, 1989), p. 649.
2. E.L. Belokoneva, N.A. Simionov, A.V. Butashin, B.V. Mill, N.V. Belov, Dokl. Akad. Nauk USSR **225**, 1385 (1980).
3. E.L. Belokoneva, N.V. Belov, Dokl. Akad. Nauk USSR **260**, 1363 (1981).
4. B.V. Mill, A.V. Butashin, G.G. Kodzhabagyan, E.L. Belokoneva, N.V. Belov, Dokl. Akad. Nauk USSR **264**, 1385 (1982).
5. A.A. Kaminskii, E.L. Belokoneva, B.V. Mill, S.E. Sarkisov, K. Kubanov, Phys. Stat. Sol. A **97**, 279 (1986).
6. R.D. Shanon, C.T. Prewitt, Acta Cryst. B **25**, 925 (1969).
7. D. Barb, S. Constantinescu, D. Tarina, I.S. Lyubutin, B.V. Mill, V.G. Terziev, T.V. Dmitrieva, A.V. Butashin, *Proc. 1st Gen. Conf. Of Balkan Phys. Soc., Thessaloniki, 1991*, edited by K.M. Paraskevopoulos (Hellenik Phys. Soc. Thessaloniki Branch), p. 800; D. Barb, S. Constantinescu, D. Tarina, Hyperfine Interact. **50**, 645 (1989); **96**, 83 (1995).
8. D. Ganguli, N. Jb. Miner. Abh. **130**, 303 (1977).
9. S. Constantinescu, S. Calogero, QSCOMP: "*Program of the ^{57}Fe Mössbauer quadrupole splitting parameters evaluation*", QCMP 172, QCPE Bulletin, Vol. 17, N° 1 (1997).
10. D. Barb, S. Constantinescu, D. Tarina, J. Phys. I France **79**, 1701 (1997).
11. R.M. Sterheimer, Phys. Rev. **80**, 102 (1950); **84**, 244 (1951); **95**, 736 (1954); **105**, 158 (1957).
12. R. Allaman, G. Donnay, Acta Cryst. B **27**, 1871 (1971).
13. D. Barb, S. Constantinescu, D. Tarina, Rom. J. Phys. **40**, 885 (1995).